International Journal of Recent Technology and Engineering (IJRTE)
ISSN: 2277-3878 (Online), Volume-8 Issue-6, March 2020

Mechanical Properties and Microstructure, in welded joints of Low and Medium Carbon Steels, Applying Rotary Friction

Víctor Alcántara Alza

Abstract: ***The effect of friction welding (FRW) in joints of medium and low carbon steels on its mechanical properties and microstructure was studied. AISI 1020 and 1045 steel bars of 12 mm diameter were used. Welding was carried out on a lathe with coupling to control the process parameters. For 1045/1045 joint, the following parameters were used: n = 1400 rpm, Friction pressure Pf = (0.8 - 1.0) MPa; Friction time (Tf) = 8 sec; Upsetting pressure (Pr) = 5 MPa; Upsetting time (Tr) = 5 sec, were used. For 1020/1045 joints the parameters that only varied were: n = (1000 - 1400) rpm; Pf = (0.7-0.8-1.0) MPa. Tensile tests were carried out on the IMSTRON UNIVERSAL machine under ASTM E8 standard. Microhardness tests were carried out on (HV) 0.5 scale, making a longitudinal and transverse scanning profile. Microscopy at the optical (OM) and electronic SEM levels, with analysis (EDS) was revealed. It was found for similar joints: a higher value of (Pf) increases the mechanical resistance (σrm), but for dissimilar joints decreases it. Welding efficiency of similar joints was 94% and for dissimilar joints 97.5% with regard to 1020 and 74% with regard to 1045. For dissimilar joints, a higher speed "n" increases σy, and σrm, with little effect on "ε". In similar joints the microhardness is maximum in the center, and for the dissimilar ones it is not. Longitudinal and transverse microhardness profiles do not follow a defined pattern with respect to Pf. For both types of joints, the microstructure shows, that FDRZ joint zone, has variable thickness and has a fully recrystallized fine-grain structure. TMAZ deformation zone, a structure of deformed grains and dark grains is observed, the latter, due to the excess carbon produced by diffusion. In both cases, no intermetallic compounds have been produced, and perlite colonies is not observed in these two zones.***

Keywords: ***carbon steels, microhardness, mechanical properties, friction welding.***

I. INTRODUCTION

Friction welding is a solid state welding method, where the movement of two wear surfaces generates enough heat that after applying a compression force below the melting temperature, the welded joint is achieved [1].

Manuscript received on March 15, 2020.
Revised Manuscript received on March 24, 2020.
Manuscript published on March 30, 2020.
* Correspondence Author
Dr. Víctor Alcántara A*., Professor, Department of Mechanical Engineer, National University, Trujillo-Peru.

This welding method is widely used within manufacturing methods, due to the advantages such as high material savings, low production time and the possibility of welding parts that are durable [2]. Likewise, friction welding is commonly used and suitable for series production, where two similar or dissimilar metals are successfully connected [3], [4].
It is a very advantageous alternative to fusion welds, which presents many defects due rapid cooling, such as porosities, residual stresses, and fatigue cracks, that start at the foot of the weld and spread through the heat affected zone (HAZ), depending on the geometry of the joint [5], [6]. All these defects or failures cannot be eliminated, but can be reduced with post welding methods that increase production costs. For this reason, solid state welding methods have been developed that mitigate these failures that can be catastrophic [7].

There are several methods of friction welding, whose application depends on the type of joint and the geometry of the pieces to be welded. In the case of joining circular bars, including pipes, the rotary friction welding (FRW) method is used. This type of welding involves the union between a stationary and a rotating member, due to the friction heat generated while undergoing high normal forces at the interface [8], distinguish the FRW method of continuous drive (direct drive).

In continuous drive friction welding, one of the parts to be welded rotates at constant speed (n), while the other is pushed toward the rotated part by sliding action. The components are joined under axial friction pressure (Pf) for a predetermined friction time (tf). Then the drive closes and the rotating component stops quickly while increasing the axial pressure at a higher upsetting pressure (Pr) for a predetermined time (Tr). In this way the parameters of the FRW weld are determined. The quality of the FRW weld joints is directly influenced by these parameters [9], [10].

Many studies on welding (FRW) in steels have been carried out. Z.Balalan and O.Ekince [11] studied the effects of rotational speed (n) on the mechanical properties of similar joints on 12mm diameter AISI 1040 steel bars applying FRW. They found that Tensile strength (σrm) decreases by approximately 12% with increasing rotational speed from 1500 rpm to 1700 rpm, and Yield strength (σy) decreases by 18%. H.Akata and M.Sahin [12] investigated the effects of dimensional differences in the union of AISI 1040 steel parts by means of rotary friction welding (FRW), determining optimal values of time and friction pressure, keeping constant the time, upsetting pressure and rotational speed.

It was found that the strength of the joint increases by increasing the friction time and pressure to a certain value and then decreasing. Maximum hardness values were found through the weld interface. They found when the diameters of the components to be joined are different, FRW welding can be considered an effective way to join components with different diameters up to a diameter ratio of 1: 3. M.
Sahin, et al. [13], complemented the previous investigation determining the tensile strength of steel joints AISI 1040, welded by FRW process. They found that the tensile strength of the welded parts is approximately 95% of the resistance with respect to the base metal and the fatigue resistance values were similar to those obtained in the base material. The impact resistance was slightly higher in the welded joints compared to the base material. The maximum hardness on the horizontal axis was located at the weld interface. M. Demouche et al. [14] investigated the effect of FRW welding parameters on the mechanical properties and microstructure of welded joints on high-alloy carbon steel bars (100Cr6). It was found that after cooling, a martensitic structure is obtained in the core and the periphery of the welded joint. The tensile strength of the welded samples increases with increasing time and friction force, up to a certain level, and then decreases again. Hardness measurements show higher hardness at the center of the weld joint compared to its periphery.

Dissimilar metals joints using fusion welding methods has very poor bond strength. The use of friction welding methods is best suited for joining different combinations of metals in today's technology. There are many investigations in this regard. Some of them will be mentioned.

Radosław W. (2016) [15], studied the effect of FRW parameters on tensile strength and microstructural properties of dissimilar joints in carbon steel AISI 1020 and ductile iron ASTM A536. It was found that as the friction force and the friction time increases, the tensile strength also increases. The maximum resistance of the welded joints was 87% with respect to the base metal. The results of the metallographic study show that the FRW welding process was accompanied by a diffusion of ductile iron carbon atoms into the steel. This process caused the formation of a carbon rich zone in the interface zone and decarburization in ductile iron near the bond interface.

S. Haribabu, et al, [16] investigated the weldability in the different combinations of AISI 304 austenitic stainless steel and AISI D3 tool steel using the FRW welding technique. The results showed that the tensile strength of the joints increases with the increase of the upsetting and friction force initially, and decreases after reaching the maximum value of 388 MPa. The microhardness of the joints increased towards the weld interface from the base metal due to the effect of strain hardening and the presence of fine grains at the interface. This weld interface is irregular and wider in the peripheral region compared to the center of the joints. This is because tangential speeds are higher at the periphery than at the center, causing different friction forces with different temperatures and different effects.

In spite the increased efficiency and benefits offered by friction welding, the trend to use fusion welding methods still continues, especially in small and medium enterprises. Therefore, the objective of this study is focused on determining the tensile mechanical properties, the longitudinal and transverse microhardness profile, as well as the microstructure of similar welded joints of Steels: AISI 1045/1045 and dissimilar joints of steels AISI: 1020 / 1045.

II. MATERIALS AND METHODS

A. Materials Used

AISI 1020 and 1045 drawn steel bars 12 mm in diameter were used. The chemical composition of the materials are found in Table I, and their microstructure in the supplied state is shown in Fig. 1

Table I. Chemical composition of the steels used

Steel	Chemical composition (% w)			
	C	Mn	P	S
AISI 1020	0.23	0.40	0.03	0.04
AISI 1045	0.43	0.80	0.03	0.04

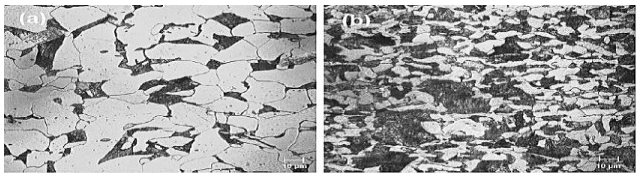

Fig. 1. Microstructure of the supplied steels: a) AISI 1020 and b) AISI 1045. Colonies of perlite (dark zone) and ferrite (white zone) are observed.

B. Equipment.

FRW welding process was carried out using a lathe, to which a mechanism was attached that allowed to control the process parameters, as shown in Fig. 2. The chuck of the lathe allowed the turning speed to be given to half of the joint, and the other half was supported by a fixed Chuck attached to the tailstock. To give the friction (Pf) and upsetting (Pr) pressure; a hydraulic jack was attached to the bed and aligned to the axis of the lathe. A calibrated manometer was attached to the hydraulic jack to measure the Pf and Pr pressures and a chronometer was attached to measure the times. The coupling mechanism was mounted and adjusted to the lathe bed to give it precision, the ability to withstand vibrations and avoid misalignment of the axis between the rotating part and the stationary part.

C. FRW welding process

Before applying FRW method, the faces of the specimens were carefully machined, to obtain a uniform weld throughout the interface area. FRW method was by “direct impulse”. One of the workpieces (left side) was clamped to the lathe chuck, rotating at the respective rpm.

Fig. 2. Conventional lathe showing details of the fixed chuck thrust coupling to perform the (FRW) tests. Coupling according to [24].

while the other (right side) remained static attached to the fixed chuk. Then the joints were coupled and rotated using the speeds, pressures of friction, forging and times, according to the parameters indicated in Table II.

During the process, the surfaces were first brought together and aligned to initiate bonding using a pressure Pf, for a time Tf. After the ring flash welded in a plastic state appeared (Fig. 2), pressure Pr was applied for a time Tr, and then the air-welded joints were cooled.

D. Tensile tests

Before performing these tests, all welded joints, both similar and dissimilar, were machined according to ASTM E8. They were machined on the MHASA lathe, reducing its diameter to Ø 9 mm in the test area, as indicated in the standard. After that, they were ground and polished with sandpaper grades: 120 and 320 to ensure tolerances for cylindricality, circularity, and roundness, in addition to checking the surface finish specifications, to avoid stress concentrators and fractures in the test area. Three replicates were made for each sample and the values obtained were averaged. All tensile tests were performed on the IMSTRON

Table II. Parámetros de Procesos: FRW

Item	FRW: 1045/1045	FRW: 1020/1045
n (rpm)	1400	1000-1400
Pf (MPa)	0,8-1,0	0,7- 0,8-1,0
Tf (s)	8	8
Pr (MPa)	5	5
Tr (s)	5	5

Velocidad Rotación (n); Presión de Fricción (Pf); Tiempo de Fricción (Tf); Presión de recalcado (Pr); Tiempo de Recalcado (Tr):

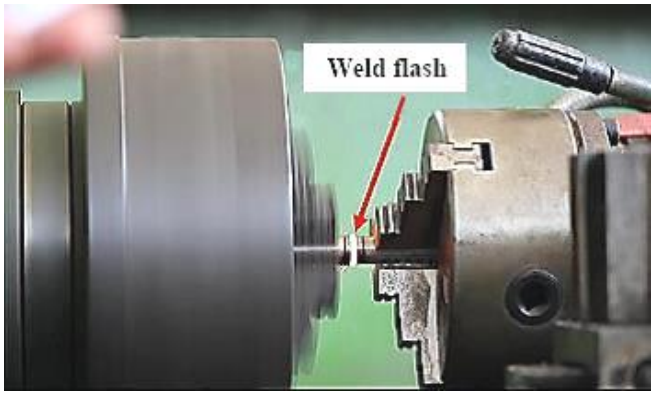

Fig. 3. FRW process test, where the plasticized layer of the weld appears at the joint interface (Weld flash), after applying friction pressure (Pf) and forging (Pr).

UNIVERSAL 8801 10 Ton capacity machine, according to the ASTM E8 standard.

E. Microhardness Tests.

Half-cylinder specimens drawn from the welded joints, were made for both types of weld. After being machined, they were ground and polished with 400, 800 sandpaper and alumina cloth. The Vickers CV400DTS microdurometer with motorized turret, digital measurement microscope and touch screen system was used. Measurements were made on scale $(HV)_{0.5}$, making a longitudinal and transverse scanning profile, according to the scheme of Fig.4.

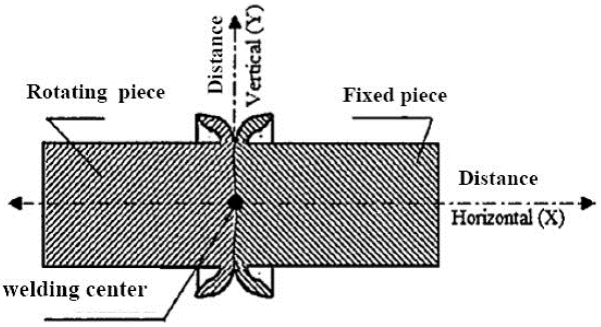

Fig. 4. Diagram specifying the directions of microhardness profiles in FRW welded joints.

F. Microscopy Test

Microscopy analysis was performed at the optical level using a ZEISS microscope, (1000X). At the electronic level, a SEM scanning electron microscope was used, mark JEOL JSM-6490LV, with an x-ray analyzer (EDS) built-in . To reveal the microstructure, the samples were ground, polished and chemically attacked. Sandpaper from grade 220 to 1000 was used, then it was polished with corduroy cloth with alumina from grade 5 µ, up to 0.3 µ and water, for 30 sec; they then were attacked with Nital 3% for 60 sec, and were ready to reveal the microstructure. With the revealed samples, it was possible to roughly estimate the dimensions of the joining areas and define the phases for each process.

III. RESULTS AND DISCUSSION

A. SIMILAR JOINTS; FRW: (AISI 1045/1045)

A1. Tensile strength: (σ_{rm})

Figure 5 shows the values of (σrm) of the welded joints. The maximum value: 772.5 MPa, corresponds to Pf = 1.0 MPa (150 psi) and Tf = 8 sec. The minimum value: 596 MPa, corresponds to Pf = 0.8 MPa (120 psi) and Tf = 8 sec. These values are in agreement with the studies by S. T. Selvamani et al. [17] carried out under similar conditions in FRW joints: AISI 1035-1035, where it is observed that "The higher the friction pressure, the mechanical resistance increases and the longer the friction time, it also increases it". This result is supported by the fact that the heat generated during friction; Although it is the parameter responsible for the union, it is not necessary to reach the melting point for the materials weld, demonstrating that it is a union that is basically produced by interatomic diffusion.

Regarding (σrm), an efficiency of 94% is found for welded joints with Pf = 1.0 MPa and 77.6% for welded joints with Pf = 0.8 MPa, demonstrating the Pf influence.

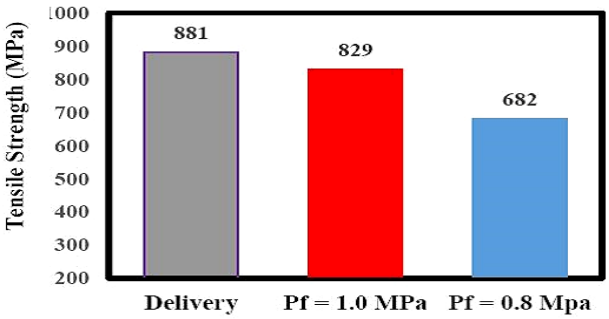

Fig. 5. Tensile strength (σrm) of welded similar joints FRW: AISI 1045/1045 for different Pf values.

A2. Microhardness Profiles.

Fig. 6a) shows the longitudinal microhardness profile for the FRW 1045/1045 joint. Its maximum value (285 HV) is in the junction zone and corresponds to Pf = 1.0 MPa. The microhardness is maximum at the interface and this may be due to the formation of brittle intermediate metals and is one of the reasons for the lower value of σrm compared to the resistance of the base metal [18]. These maximum values found in the center of the union; and are explained by the fact that this area is totally deformed and therefore very hardened.

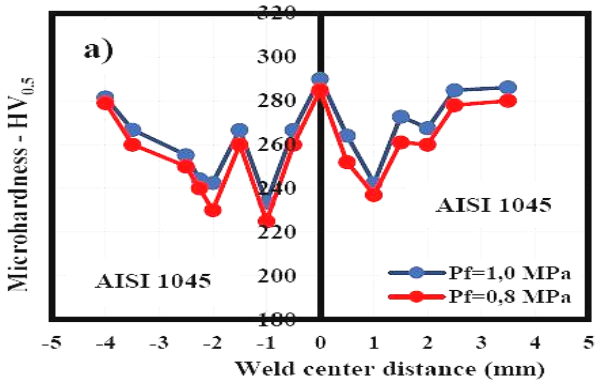

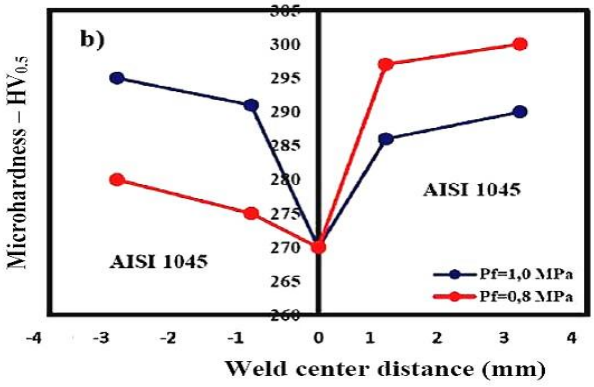

Fig. 6. FRW joint microhardness profiles: AISI 1045/1045 with different friction pressures. a) Longitudinal profile; b) Transverse profile.

It is the (FPDZ) area, of very fine grain where hard and fragile structures are produced, because the FRW welding itself is a process that affects the material mechanically and thermally. The same does not occur with transverse hardness where the minimum value (270 HV) is located in the center of the joint, increasing to a maximum (320 HV) when reaching the periphery of the sample. These results are explained based on the fact that the linear speed increases from the center to the surface. Therefore, depending on the speed, in the welding zone the temperature at the center is minimum, while the temperature at the far end is maximum. The structural change takes place in relation to these speeds and temperature changes [19].

B. DISSIMILAR JOINTS : FRW (AISI 1020/1045)

B1. Tensile Test Results.

The results are shown in Table III, and their corresponding curves stress-strain (σ-ε) are observed in Fig. 7. In each graph, the curves (σ-ε) of the joints are shown as a function of the rotation speed (n) and friction pressure (Pf). The other parameters remain constant.

Table III. Tensile Mechanical Properties of dissimilar welded joints FRW: AISI 1020/1045

RPM	PRESIÓN DE FRICCIÓN (MPa)								
	Pf= 0.7 MPa			Pf = 0.8 MPa			Pf = 1.0 MPa		
	σ_Y (MPa)	σ_{max} (MPa)	ε (%)	σ_Y (MPa)	σ_{mx} (MPa)	ε (%)	σ_Y (MPa)	σ_{max} (MPa)	ε (%)
1400	585	630	12.5	510	550	7,7	480	520	7,5
1000	573	625	10,3	450	540	7,8	500	510	7,5
AISI 1020 suministro	617	646	23,5	-	-	-	-	-	-
AISI 1045 suministro	750	850	17,0	-	-	-	-	-	-

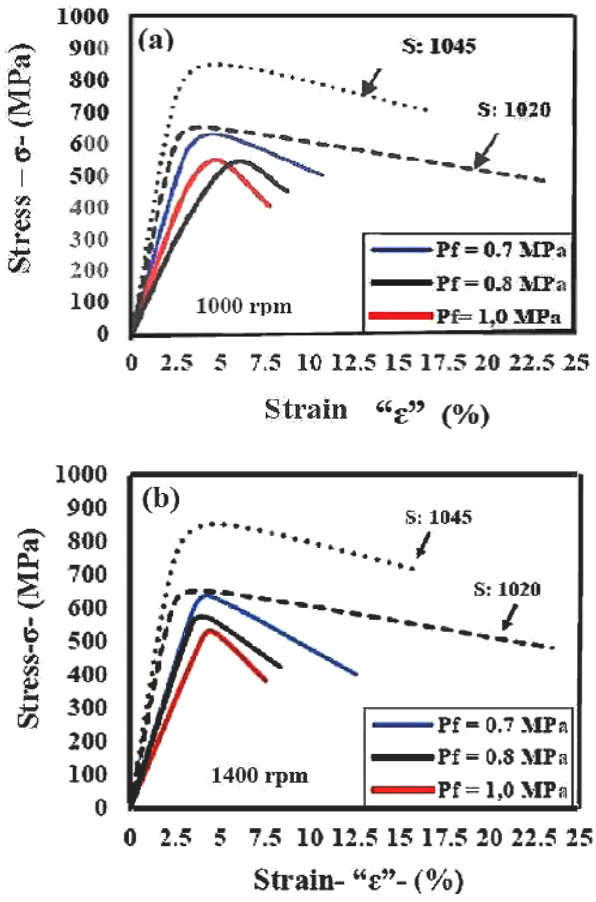

Fig. 7. Diagrams (σ-ε), of the welded joints FRW: AISI 1020-1045, with different "Pf" and "n"; (a) 1000 rpm, (b) 1400 rpm. The curves with dashed lines correspond to the base materials.

It is observed that for the two rotational speeds, the yield limit (σy) and the mechanical resistance (σmax) decrease as increases (Pf). For 1000 rpm the maximum tensile efficiency was 97.5% compared to AISI 1020 and 74% compared to AISI 1045, both achieved with Pf = 0.7 MPa.

The elongation is almost unchanged with the rotation speed (n), but it decreases if Pf increases. Its maximum value was 12.5% for n = 1400 rpm and Pf = 0.7 MPa. The minimum was 7.5% for the two speeds with Pf = 1.0 MPa; but taking into account the base materials; the ductility of the joint decreases to a third with respect to AISI 1020 and approximately to half with respect to AISI 1045.

B2. Microhardness Profiles.

Fig 8 shown the longitudinal microhardness profiles. It is observed for the two rotational speeds that the hardness in the center of the bead is greater than zone corresponding to 1020 steel, but less than corresponding to 1045 steel. Fig. 8a) shown the profiles for samples with 1000 rpm; whence it follows that the total zone of welding and deformation measure ~ 12 mm, sharing 6 mm for both sides; the same happens for samples with 1400 rpm (Fig. 8b). In both cases the microhardness is in the range ~ (150 - 320) $HV_{0.5}$. No definite relationship is found between microhardness and Pf.

Transverse microhardness profiles are shown in Fig. 9. In Fig. 9a) we have the profiles for samples with 1000 rpm, where a maximum value (320 HV) is observed, located 4 mm up the center of the cord and a minimum value (230.2 MPa), located at the center of the chord, both values for Pf = 0.8 MPa. The profiles show an irregular behavior with the penetration. At 14000 rpm, irregular curves ranging from ~ (240-300) HV are also observed; that is, for a distance of 5 mm, a variation in hardness of ~ 60 HV occurs from the center of the bead, an almost negligible variation in practice.

Microhardness profiles, both longitudinal and transverse, do not follow a defined pattern of behavior with respect to the friction pressure Pf and the trends are oscillating for the two types of profiles. Therefore, it can be affirmed that there is no defined relationship between microhardness and Pf.

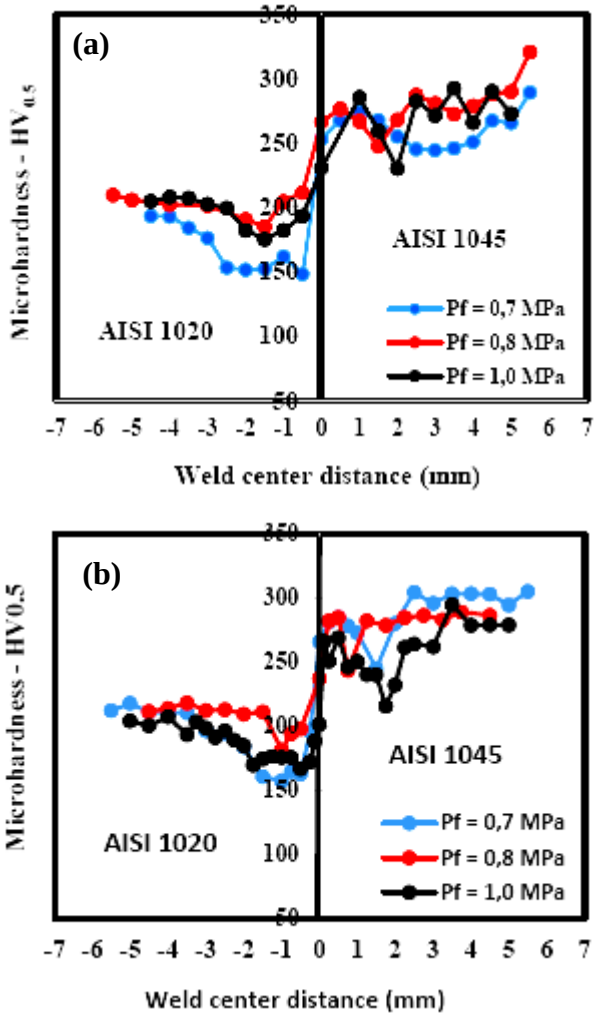

Fig. 8. Microhardness profiles Longitudinal of the FRW joint: AISI 1020/1045 for various friction pressures (Pf) and two speeds; (a) 1000 rpm; (b) 1400 rpm.

C. MICROSTRUCTURE

Materials near the interface are divided into three different zones, 1) The dynamic fully recrystallized zone (FDRZ), 2) The mechanically and thermally affected zone, and (TMAZ)

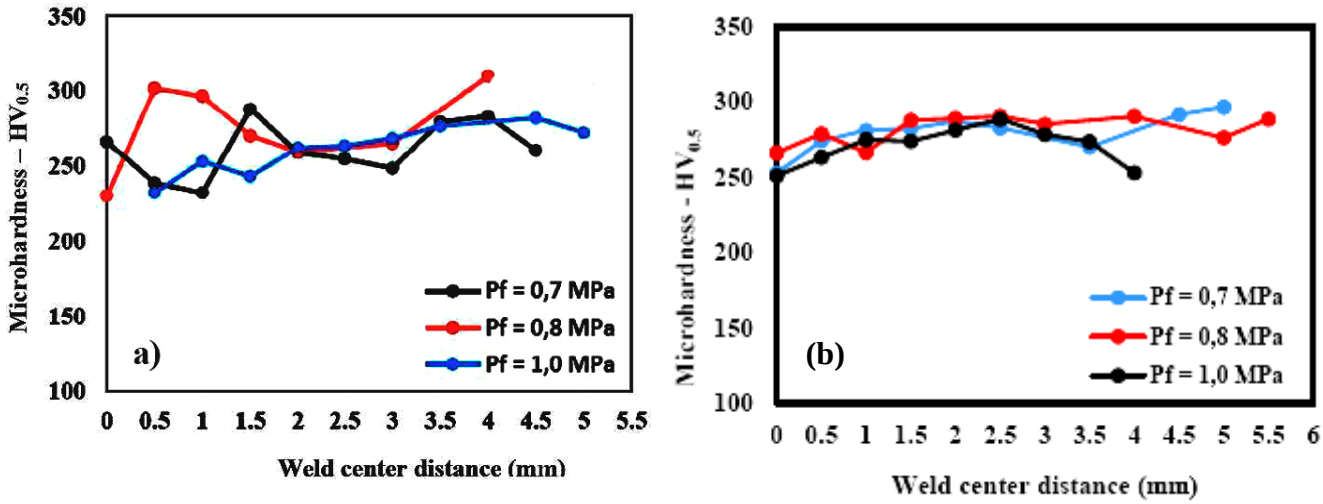

Fig. 9. Microhardness profiles transverse of the FRW joint: AISI 1020/1045 for various friction pressures (Pf) and two speeds; (a) 1000 rpm; (b) 1400 rpm.

3) The heat affected zone (HAZ). [20] - [22]. In Fig. 10 these zones are observed for a FRW 1045/1045 joint (1400 rpm and Pf = 1.0 MPa).

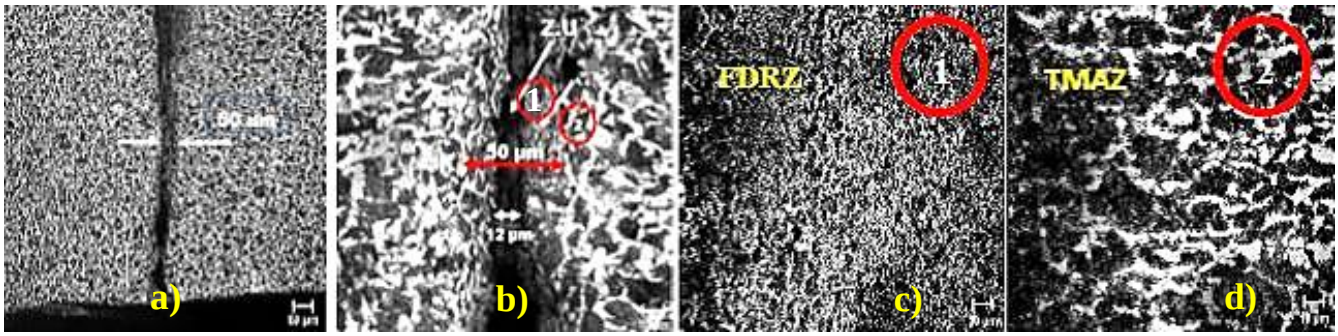

Fig.10. Optical Microstructure (OM) of FRW 1045/1045 welded joint for: n = 1400 rpm and Pf = 1.0 MPa; a) shows the join thickness ~ 50 µm; b) micrograph at higher magnification indicating the areas attached to the joint zone (Z.U); c) Zone closest to the union, totally recrystallized (FDRZ); d) Zone mechanilly and thermically affected (TMAZ).

C1. SEM MICROSCOPY – WELDED JOINT: (AISI 1045/1045)

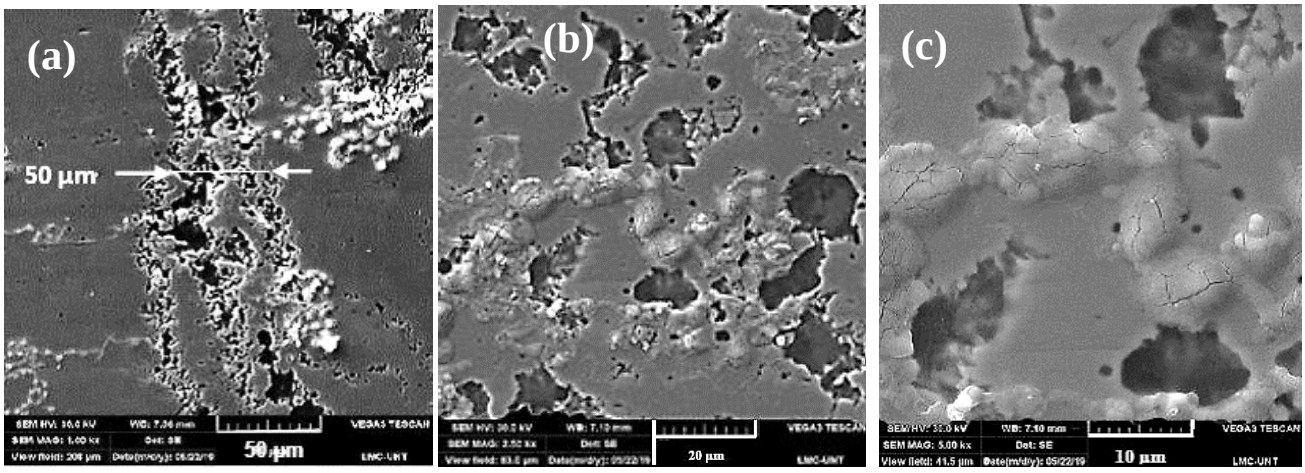

Fig. 11. SEM photomicrographs of the joint center (interfaz) of the FRW 1045/1045 weld at various magnifications. a) An average of 50 µm of joint thickness is observed. b) Globules of deformed material and carbon clusters are observed. c) Deformations seen at higher magnification. No pearlitic structures are observed Parameters: [1400 rpm; Mp = 1.0 Mpa]

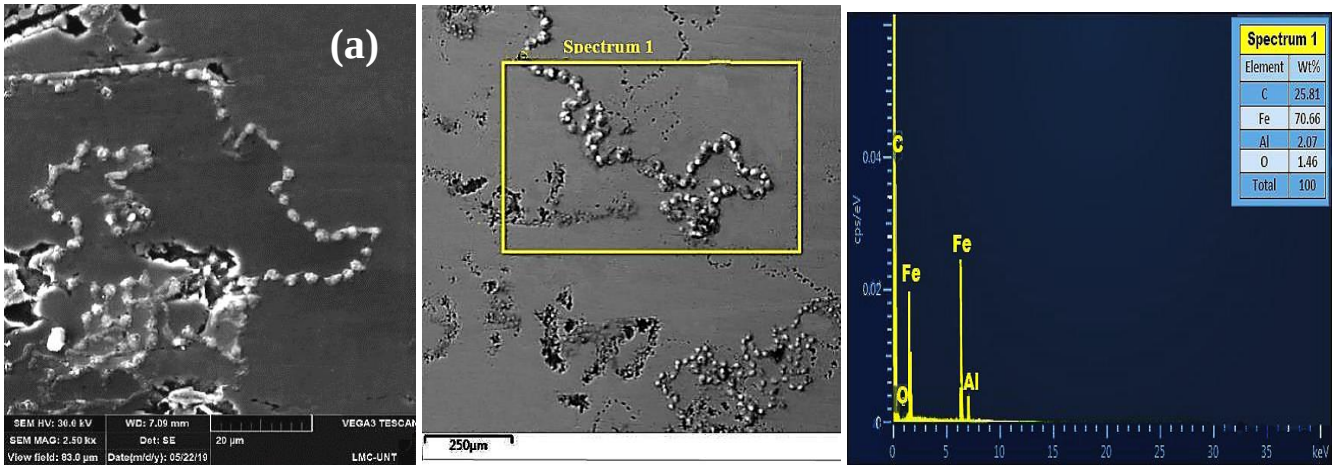

Fig. 12. SEM micrographs taken 1mm right of FRW 1045/1045 weld interface (TMAZ); a) String of globules formed by the effect of deformation; b) Location area for analysis; c) EDS analysis of the marked area. Parameters: [n = 1400 rpm: Pf = 1.0 MPa]

In Figure 10, the microstructure of the areas that make up the weld bead of the FRW 1045/1045 joints is observed at the optical level. The average bead thickness ~ 50 µm can be observed (Figs. 10a and 10b) and in more detail the FRDZ and TMAZ zones. In the first one (Fig. 10c), a fine-grained structure distributed uniformly is observed, as a result of the total recrystallization produced in that area. In the second one (Fig. 10d), an elongated grain structure with equiaxial dark areas is observed due to the effect of deformation and partial recrystallization.

In Figures 11, the structure of the junction zone (Z.U) of FRW 1045/1045 is shown at the SEM level. Fig. 11a) shows in detail the irregular profile of this area, with an average thickness of ~ 50 µm, according to fig. 10b). The profile shows well defined junction areas and dark areas, which may be carbon clusters, along with colonies of white globules. In Figs. (11b) and 11c) at higher magnifications, it is observed that the globules are grains deformed by the effect of forging pressure (Pr) and the carbon clusters are iron (α) grains supersaturated of carbon, which have migrated towards these zones by effect of diffusion. This statement is supported by measurements of temperatures at the interface, together with metallographic studies done in other studies where it has been concluded that diffusion is a primary mechanism in friction welding [23]. This is aided by the clean action of relative motion, the applied Pf, along with the forging pressure (Pr).

In Fig. 12, it has being a micrograph taken 1 mm to the right of the junction zone that corresponds to the TMAZ zone. These globules are also found to be in the thermally and mechanically affected zone. The EDS test indicates that they are Fe-C compounds, and the globular shape is explained by the deformation produced in the process. The EDS indicates that there has been no intermetallic compound and it cannot be stated that the dark phases with grain appearance are colonies of perlite and / or cementite. The composition shown in the EDS analysis does not correspond to these phases. .

C2. SEM MICROSCOPY – JOINT: (AISI /1020/1045)

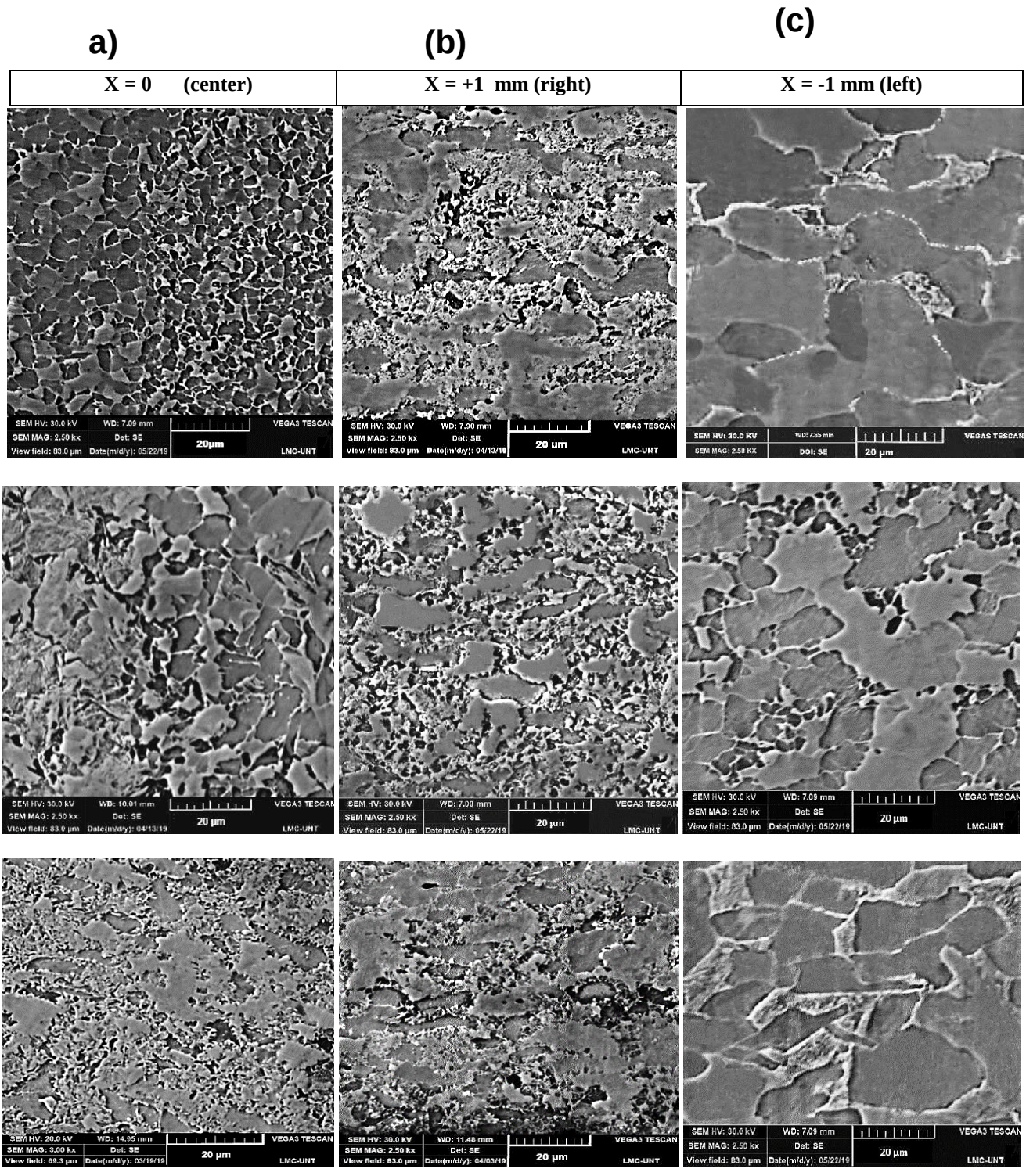

Fig. 13. SEM photomicrograph of the dissimilar joint FRW 1020/1045; (a), (b), (c): [1000 rpm; Mp = 0.7 MPa] (d), (e), (f): [1400 rpm; Mp = 0.7 MPa]; g) h) i): [1400 rpm; 0.8 MPa]. The microstructures are located in the following order: On the left they correspond to the union zone, to the center to AISI 1045 steel and to the extreme

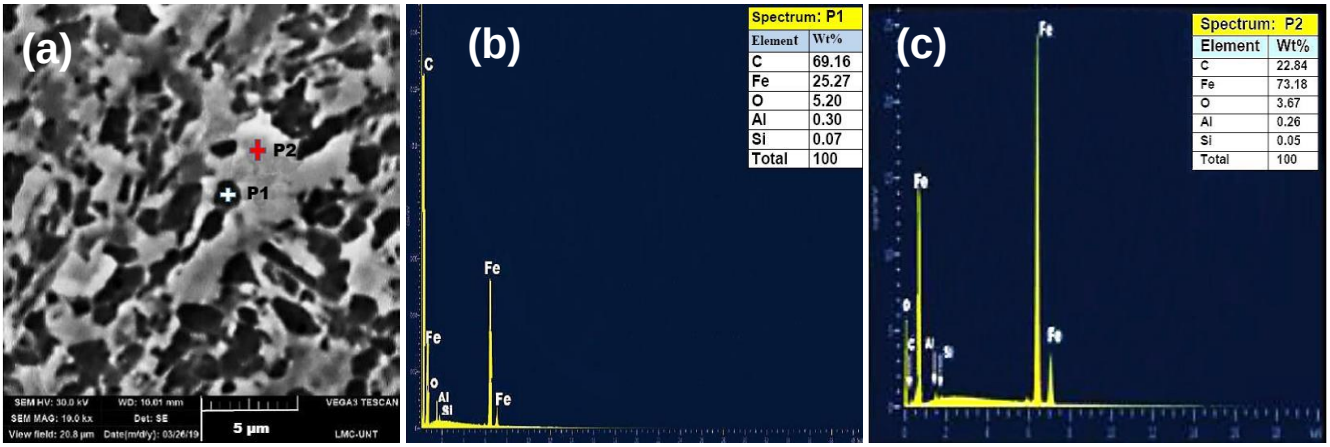

Fig. 14. SEM micrographs taken 1 mm to the right of the FRW 1020/1045 joint interface, [n = 1400 rpm: Pf = 0.8 MPa]; a) Extended area locating 2 points for composition analysis; b) EDS for point 1; c) EDS for point 2.

In Fig 11a), it is also observed that the width of the interface region varies from the center to the periphery where it is enlarged because the radial speed is greater at the ends, which can lead to different microstructures. It has been shown that the width of this zone also increases with the increase in Pf [25].

In Fig. 13, the microstructures of the welded joints with dissimilar materials are shown, FRW 1020/1045. Each row indicates three welding conditions and each column its location. In Figs. 12 a), d), g,), we have the left column that corresponds to the Z.U zone of the welded joints. A structure of totally recrystallized grains of the equiaxial type is observed, but of different sizes. The finest grain is observed in Fig. 12a), obtained with (1000 rpm, Pf = 0.7 MPa) and the coarsest in Fig. 13g) with (1400 rpm, Pf = 0.8 MPa). The most severe condition increases the size of the grain, a situation opposite to that of similar joints; because they are two different materials with different physico-chemical properties. In Table III is observed, the difference in mechanical properties does not vary much with these changes in the parameters used. The samples in Fig. 12 b), e) h) are located 1 mm to the right of the center (central column) and correspond to the TMAZ zone of AISI 1045. Different types of grains, deformed and thickened, can be seen in this area. This zone is said to correspond to partial recrystallization resulting in fewer recrystallized grains, and showing many more deformed grains. In Fig. 12 c) f) i), the TMAZ zone corresponding to AISI 1020 is observed; the same characteristics are observed, but with much larger grains than in the case of AISI 1045 steel.

In Fig 14a) an amplified sample from Fig 13 h) has been chosen in order to determine the structure of the dark and light areas. The EDS analysis has been performed for two points (1 and 2) located in those areas. The EDS analysis for point 1 (Fig. 14b) indicates an Fe-C structure, with excess carbon and for point 2 (Fig 14c) an Fe-C structure with carbon depletion. Perlitic ferritic zones are not observed, nor the formation of intermetallic compounds. This is due to the diffusion that has produced an excess of carbon concentration in the dark areas and a carbon deficit in the light areas with an almost Fe-α structure.

Unlike the microstructure shown in Fig 11 where the Z.U. of the similar joint FR 1045/1045 it is clearly seen; The same does not happen with the dissimilar FRW dissimilar 1020/1045 joint, where the Z.U, being an intermix, is not entirely clear, due to the carbon diffusion from 1045 to 1020; but it should be taken into account, that the width of the intermixing zone decides the mechanical performance of these welds [26].

IV. CONCLUSION

The conclusions of present study can be synthesized in the following points:

1. For similar 1045/1045 joints a higher value of (Pf) increases the mechanical resistance (σrm), but for dissimilar joints, the increase in Pf decreases it slightly. At similar joints, a tensile efficiency of 94% was obtained. For dissimilar boards 97.5% compared to 1020 and 74% compared to 1045.
2. For dissimilar 1020/1045 joints, a higher rotation speed increases σy, and σrm, with little effect on "ε"; but these values are significant with respect to the base materials. The ductility of the joint decreases almost a third compared to 1020 and half compared to 1045.
3. For similar joints, the microhardness has maximum values in the center. If Pf decreases, the microhardness also decreases. For dissimilar joints, the maximum values are not in the center. They are found in the area corresponding to 1045. The microhardness profiles, longitudinal and transverse, do not follow a defined pattern with respect to Pf.
4. Regarding the microstructure; in the FDRZ zone, for the types of joints, a variable thickness is observed that shows a fully recrystallized fine-grained structure. In the TMAZ zone, a structure of light elongated grains and very dark equiaxial phases is observed. The EDS analysis shows that the dark structures are compounds of Fe-α supersaturated of carbon, the one that has migrated towards those

zones due to the effect of diffusion, leaving the areas clear with carbon depletion.

5. For both the similar and dissimilar joints, in the studied zones: FDRZ and TMAZ, no intermetallic compound has been produced and neither there are colonies of perlite and /or cementite. The composition shown in EDS analysis does not correspond to these phases.

REFERENCES

1. Y. Zhou, Z. Li, L Hu, A. Fuji, TH North., Mechanical Properties of Particulate MMO/AISl304 Friction Joints. *ISIJ International*, Vol. 35, No. 10, 1315–1321, 1995.
2. M. Sahin, Evaluation of the joint-interface properties of austenitic-stainless steels (AISI 304) joined by friction welding, *Materials and Design* 28 (2007) 2244–2250
3. 3. M. Gurler. "Friction welding characteristics of aluminum alloy". PhD. Thesis. Marmara University, Institute of Science, Istanbul; 2000.
4. I. Kırık, N. Ozdemir. "Microstructure and mechanical behaviour of friction welded AISI 2205/AISI 1040 steel joints*". Mater Test* 2012; 54(10):683–7
5. J. Barsom y S. Rolfe, "Fracture and Fatiigue Control in Structures: Applications of Fracture Mechanics", third edition, ASTM Stock Number: MNL41, USA, 1999.
6. D.F.Atehortua-López., "Propagación de grietas en uniones soldadas por FCAW de aceros de bajo carbono y aceros de baja aleación", PhD. Tesis, Facultad de Ingeniería, Universidad del Valle, Cali, Colombia, 2016
7. M. Uzkut, B. Unlu, S. Yilmaz, M. Akdağ.; "Friction Welding and Its Applications in Today´s World". Disponible http://eprints.ibu.edu.ba/621/1/issd2010_science_book_p710-p724.pdf
8. ASM Handbook Committee (1971) Welding and brazing, 8th edn, vol 6. American Society for Metals
9. H. Mesmari, F. Krayem, Mechanical and Microstructure Properties of 304 Stainless Steel Friction Welded Joint, *International Research Journal of Engineering Science, Technology and Innovation (IRJESTI)* Vol. 2(4) pp. 65-74, July, 2013
10. Kinley W (1979) Inertia welding: simple in principle and application. *Weld Met Fabr* 10:585–589
11. 11. Zulkuf Balalan and Omer Ekinci, Effect of Rotation Speed Parameter on Mechanical Properties of Similar AISI 1040 Parts Joined by Friction Welding, *Metallofiz. Noveishie Tekhnol.*, **40**, No.12: 1699–1707 (2018), DOI: 10.15407/mfint.40.12.1699.
12. 12. H. Akata, M. Sahin, "An investigation on the effect of dimensional diferences in friction welding of AISI 1040 specimens" *Industrial Lubrication and Tribology*, 2003.
13. 13. M. Sahin, H. Akata y T. Gulmez, "Characterizacion of mechanical properties in AISI 1040 parts welded by friction welding", *Materials Characterization*, Volume 58, p.p 1033-1038, September 2006.
14. 14. M. Demouche1, E. H. Ouakdi, R. Louahdi, Effect of Welding Parameters on the Microstructure and Mechanical Properties of Friction-Welded Joints of 100Cr6 Steel, *Iranian Journal of Materials Science & Engineering* Vol. 16, No. 3, September 2019. DOI: 10.22068/ijmse.16.2.24
15. 15. W. Radosław. "Effect of friction welding parameters on the tensile strength and microstructural properties of dissimilar AISI 1020-ASTM A536 joints", *Int J Adv Manuf Technol* (2016) 84:941–955.
16. 16. S. Haribabu, M. Cheepu, L. Tammineni, N. Gurasala, V. Devuri and V. Kantumuchu., Dissimilar Friction Welding of AISI 304 Austenitic Stainless Steel and AISI D3 Tool Steel: Mechanical Properties and Microstructural Characterization, Advances in Materials and Metallurgy, Lecture Notes in Mechanical Engineering,
17. DOI: https://doi.org/10.1007/978-981-13-1780-4_27
18. 17. S.T. Selvamani, K. Palanikumar, Optimizing the friction welding parameters to attain maximum tensile strength in AISI 1035 grade carbon steel rods, *Measurement* (2014),
19. DOI:http://dx.doi.org/10.1016/ j.measurement.2014.03.008
20. 18. N. Mathiazhagan1, T. Senthil kumar, Effect of mechanical properties and microstructure on medium carbon steel using friction welding, International Conference on Energy Efficient Technologies For Automobiles (EETA' 15) ISSN: 0974-2115
21. 19. A.Z. Sahin, BS Yibas, M. Ahmed, J. Nickel., Analysis of the friction welding process in relation to the welding of copper and steel bars. *J Mater Process Technol* 1998; 82:127–36.
22. 20. F. D. Duffin and A. S. Bahrani: Frictional behaviour of mild steel in friction welding, *Wear*, 1973, 26, 53–74.
23. 21. O. T. Midling and Ø. Grong: A process model for friction welding of A1-Mg-Si alloys and A1-SiC Metal matrix composites—I, Haz temperature and strain rate distribution, *Acta Metall. Mater.*, 1994, 42, (5), 1595–1609
24. 22. O. T. Midling and Ø. Grong: A process model for friction welding of A1-Mg-Si alloys and A1-SiC metal matrix composites--II. Haz microstructure and strength evolution, *Acta Metall. Mater.*, 1994, 42, (5), 1611–1622.
25. 23. M. Maalekian (2007) Friction welding – critical assessment of literature, Science and Technology of Welding and Joining, 12:8, 738-759,
26. DOI: 10.1179/174329307X249333
27. 24. A. Handa and V. Chawla, Experimental evaluation of mechanical properties of friction welded AISI steels, Handa & Chawla, *Cogent Engineering* (2014), 1: 936996
28. 25. M. Cheepu; W. Che, Influence of Friction Pressure on Microstructure and Joining Phenomena of Dissimilar Joints, *The Indian Institute of Metals* - IIM 2020.
29. DOI: https://doi.org/10.1007/s12666-020-01908-w
30. 26. L. Peng, P. Longwei, H. Xiaohu, L. Shuai, and D. Honggang, Effect of post-weld heat treatment on inhomogeneity of aluminum/copper rotary friction welded joint, *Mater Res Express* (2018) 5 096504.

AUTHOR PROFILE

Dr. Víctor Alcántara A. working as a professor in Mechanical Engineer Deparment of the National University of Trujillo-Peru. Mechanical engineer, Master in Materials Engineering (1996) and Doctor in Materials Science (2006) Lima-Peru. Member of the Materials Research Institute of the Post Graduate School at the National University of Trujillo. Specialization in characterization of ferrous and non-ferrous materials, carried out at the University of Cartagena of Spain. Author of multiple manuals and texts on materials and manufacturing processes. International speaker at multiple conferences in the Latin American region. Author of several articles in indexed journals